IMAGE-BASED MULTIFUNCTION INSTRUMENT FOR AUTOMATED NONWOVEN WEB STRUCTURE ANALYSIS

R. R. Bresee and Z. Yan
The University of Tennessee
Knoxville, TN

Abstract

Image analysis hardware and software techniques are used to characterize the structure of nonwoven webs. Hardware is discussed first and emphasis is placed on selecting hardware to accommodate a variety of web structures. Software is discussed next and emphasis is placed on automating the analysis procedure. Examples of web structure measured by image analysis also will be discussed.

Introduction

The properties of nonwoven webs result from two general things - the properties of fibers in the web and the way fibers are assembled in the web (web structure). That is, knowledge of web structure is generally necessary to understand web properties. In addition, it is necessary to have knowledge of the variation in web structure to understand some web properties such as strength and filtration performance. Most people would agree that relatively little structural information is usually obtained for nonwoven materials and variations in web structure are rarely measured.

Advances in personal computers, video cameras and motion control devices have been impressive during the last two decades. Successful uses of computer vision techniques in diverse areas such as advertising and military applications lead us to expect that image-based techniques may be successfully used to obtain detailed information about web structure in the off-line laboratory environment or the on-line production environment.

Nonwoven webs generally exhibit relatively poor uniformity compared to other textile materials and natural fibers generally exhibit less uniformity than man-made fibers. As a result, a large number of measurements must be obtained to estimate web structure with reasonable precision and confidence. Automating the measurement procedure is required to obtain a large amount of data in a practical manner. We have previously published reports describing analysis of images acquired from nonwoven webs using visible light imaging (Yan and Bresee 1999). The software tools developed in our laboratory can be used to characterize most major web structural features and many web defects. Analysis modules developed for thin webs include pores (Huang and Bresee 1993a), fiber orientation (Huang and Bresee 1993b), fiber bundle diameter (Huang and Bresee 1993b) and single fiber diameter (Huang and Bresee 1994). Analysis modules developed for any web include basis weight uniformity (Huang and Bresee 1993c) and bright/dark defects (Huang and Bresee 1993c).

These analysis modules share many common features in hardware and software. For example, they share a computer, camera, image grabber and display device. They also share software functions such as size calibration, file utilities, printing, statistical analysis and producing/editing data charts. Consequently, it is cost effective to integrate all analysis tools into a single instrument system. We have accomplished this task and have briefly described some aspects of our whole instrument system (Yan and Bresee 1999). When a variety of different analysis tools are integrated into one instrument, considerable effort is required to achieve enough instrument flexibility to accommodate a reasonable variety of web structures, lenses and illumination. For example, relatively high magnification lenses are required to spatially resolve some structural features in nonwoven webs so microscope objective lenses must be accommodated by the instrument. On the other hand, relatively low magnification lenses are required for other measurements so ordinary camera lenses also must be accommodated. Since these lenses are quite different, support structures and illumination sources must be flexible.

We developed a flexible computer-controlled multifunctional instrument based on image processing and pattern recognition techniques that is dedicated to automated nonwoven web structural analysis. The instrument design is flexible in terms of lens selection, illumination and web sampling schemes. This flexibility allows a wide range of web structural features from many types of webs to be measured with a single instrument. This instrument provides us with *automated* control of sample positioning, focusing, image acquisition, image processing and image analysis. This instrument has proven to be convenient for performing unattended time-consuming analysis schemes, extensive sampling of webs and edge-to-edge analysis of large webs. Structural features measured by our instrument are summarized in Table 1.

Image Analysis Hardware

Relatively inexpensive yet powerful image analysis hardware can be assembled using mostly commercially available components. Figure 1 shows a schematic illustration of the basic hardware system we currently use. Major components consist of a desktop personal computer, monochrome frame grabber board installed in the computer, system monitor, CCD video camera, video monitor, XY table, focusing motor and light source. The video camera and frame grabber acquire images with 640x480 pixel spatial resolution and 8-bit (256 gray levels) gray level resolution.

Basic operation of the automated instrument involves placing a nonwoven web on the table, selecting a test, entering settings for the test (total number of images to be acquired, web locations of the acquired images, etc.) and then starting the program. Once the program begins, it continues without human intervention until the preset number of web locations or objects have been analyzed. Then, a statistical summary of analysis results and a data chart are ready to display and print.

Our XY table accommodates webs as large as 24inch x 24inch. Autofocusing is required for large web samples since it is difficult to maintain optical flatness over a large area. The shaft of a microstepper motor is coupled directly to the microscope fine focus shaft and yields a minimum linear lens movement (focus) of 0.01 um. We developed software to allow automated focusing at low and high magnifications and focusing is placed entirely under programming control so it is performed automatically prior to image acquisition. This feature allows individual objects within a high magnification image to be individually focused or a whole web within a low magnification image to be optimally focused.

Lens selection markedly influences image quality and appropriate illumination is always critical to imaging applications. To guide lens and illumination selection, we can consult well-known equations describing image quality (Inoue 1986), emphasizing lateral spatial resolution, depth-of-field and image contrast. The minimum lateral distance (d) in a specimen that can be resolved by conventional diffraction-limited optical microscopy can be given by

$$d = 1.22\,\lambda\,/(\mathrm{NA}_{\mathrm{obj}} + \mathrm{NA}_{\mathrm{cond}}) \qquad (1)$$

where λ is illumination wavelength, NA_{obj} is the numerical aperture of the objective lens used to image the sample and NA_{cond} is the numerical aperture of the illumination. In this equation, a smaller d represents greater resolving power. Numerical aperture is defined as

$$NA = n \sin\theta \qquad (2)$$

Reprinted from the *Proceedings of the Beltwide Cotton Conference*
Volume 1:667-673 (2001)
National Cotton Council, Memphis TN

where *n* is the refractive index of the medium between the sample and lens and *2* is the half angle of the cone of light entering or emerging from the lens. Equations 1 and 2 indicate that lateral spatial resolution is influenced by both lens selection (NA_{obj}) and illumination (λ and NA_{cond}).

Axial spatial resolution is usually expressed in terms of its inverse, depth-of-field. Depth-of-field can be defined in terms of "setting accuracy" (2ξ) along the axis of the microscope

$$2\xi = \lambda / \{ 4n \sin^2(\theta / 2) \} \quad (3)$$

In this equation, a larger 2ξ represents greater depth-of-field (less axial resolution). This equation indicates that depth-of-field is also influenced by objective lens selection and illumination.

Image contrast is influenced by many factors, including objective lens selection and illumination. For example, changing the angular range (*2*) of light illuminating an object changes the distribution of light on the object and hence its visual appearance. In other words, image contrast is influenced by NA_{cond} .

The ability to control image quality by NA_{obj}, NA_{cond} and λ is considerable. Figure 2 shows an example of the influence of objective lens NA on image quality. Both images were acquired from the same web area using the same hardware with identical λ and NA_{cond} but 2A was acquired with a NA_{obj}=0.4 objective lens whereas 2B was acquired with a NA_{obj}=0.5 objective lens. Even though the difference in NA_{obj} is small, 2A exhibits more depth-of-field and 2B exhibits more overall image sharpness.

Figure 3 shows an example of the influence of illumination NA on image quality. Both images were acquired from the same web area using the same hardware with identical NA_{obj} and λ but 3A was acquired with a smaller NA_{cond} whereas 3B was acquired with a larger NA_{cond}. Image 3A exhibits more depth-of-field and more contrast whereas 3B exhibits more lateral resolution.

Figure 4 shows an example of the influence of illumination wavelength on image quality. Both images were acquired from the same web area using the same hardware with identical NA_{obj} and NA_{cond} but 4A was acquired with λ = 486 nm (blue) whereas 4B was acquired with λ = 656 nm (red) illumination. Even though the difference in λ is not large, 4B exhibits more depth-of-field than 4A.

Achieving proper illumination for different analysis procedures and a wide variety of web structures using a single instrument is challenging since the size of the illumination area may differ substantially. We found that only two illumination devices are needed to provide enough flexibility to illuminate nearly any web in a way that is appropriate for any of the web analysis modules used in our laboratory.

An ordinary microscope lamp/condenser lens assembly focuses light onto a small area and is used to illuminate webs when relatively high magnification images are acquired using microscope objective lenses. All original illumination features of the microscope are retained including the ability to continuously adjust illumination intensity, add filters to vary the illumination wavelength, focus the condenser lens onto the web sample, center the condenser lens with the objective lens and vary NA_{cond} by changing the condenser diaphragm aperture size.

When relatively low magnification images are acquired using an ordinary camera lens, a light source that illuminates a larger area than is possible with a microscope lamp/condenser lens assembly is required. We fabricated a simple diffused light source consisting of a box containing several light bulbs connected to a rheostat to obtain continuously adjustable brightness. Filters can be placed over the box to vary the illumination wavelength. The angle of light illuminating webs can be varied through a substantial range by changing the distance between the web and light source. When this distance is short, highly diffused illumination is directed onto the web and lateral resolution is maximized, depth-of-field is minimized and image contrast is minimized for a given lens and *f-number*. When this distance is increased, the angular range of light directed onto the sample is reduced and lateral resolution decreases, depth-of-field increases and image contrast increases.

Software Design

We designed software to measure various web structural features, accommodate various web sampling schemes and achieve full automation. Three major software functions were developed to implement full automation - an interface to allow users to specify control parameters, a flexible XY position control procedure and autofocusing. A software setting function was created to serve as a user interface to input various control parameters such as the total number of samples, distance between samples and type of sampling. Two XY positioning schemes were created to control web sampling - regular and random. Random sampling provides statistical advantages whereas regular sampling is useful when a web is sampled across its entire width. Lens focusing prior to acquiring images is necessary to obtain sharp images and accurate measurements so lens focusing is generally performed before each new image is acquired if the sample has been moved to a new position.

Humans focus a microscope lens by visually scanning images while altering the lens-to-object distance until sharpness and clarity are optimized. Computer-based autofocusing techniques work in a similar way by acquiring an image and then computing a "focus index" based on some particular autofocusing algorithm. Then, the lens-to-object distance is changed, the focus index is recomputed and the lens position corresponding to the optimum focus index value is considered to be the lens position for best focus. We developed a focus index designed to attain high speed in a practical web analysis instrument

$$F = \sum_i \sum_j \left| g(i, j) - g(i, j-1) \right| \quad (4)$$

where j is selected from among 2-N and is the pixel in a peak position where the gradient changes its sign and i is selected from among 1-M in an image of size N×M. Figure 5 shows focus index values for 33 images acquired with 50um between images from a position of out-of-focus to sharp focus and then again to out-of-focus. The images also were evaluated subjectively using the human eye to identify the step at which sharpest focus occurred and this position was identified to be images 16-17 (vertical lines in the figure). The focus index function is nearly symmetrical and unimodal and positions identified to be most sharply focused using the focus index algorithm are in agreement with steps 16-17 identified using human vision. At positions well away from sharp focus, index values continued to change.

We found that web structure influences the range of focus index values measured so we included an initial learning process that determines focus index information for a web and uses this information for all later searching activities. This makes the system more robust to a wide variety of web structures and reduces errors and increases system reliability. This algorithm has proven to be useful for maximizing the focus of whole web images.

Measuring single fiber diameter presents a different focusing problem since only part of the content of any particular image is of interest at one time and fibers in the whole image are not focused simultaneously. Figure 6A shows a typical image acquired from a web to measure single fiber diameter. The pattern used to identify focused fibers can be explained by Figure 6B which

shows a gray level profile corresponding to the line B-E in Figure 6A. The line B-E crosses two fibers - one is sharply focused whereas the other is not sharply focused. A typical fiber exhibits four edges when focused and the gray level gradient at the edges of a sharply focused fiber should be large as shown for the fiber intersecting the left portion of B-E. If measured gradient values exceed a threshold value, it is concluded that at least one sharply focused fiber is present in the image.

Nonwoven Web Measurements

Fiber diameter influences numerous web properties including porosity, filtration efficiency and mechanical properties. Even when webs have the same average fiber diameter, differences in their fiber diameter distributions may influence web properties so it is desirable to have a convenient way to measure the diameter of enough fibers to adequately characterize the diameter distribution. It also is desirable to sample fibers through the entire web thickness and to obtain multiple measurements for each fiber to average variations with individual fibers. More measurements are required when fiber diameters in a web are more variable. Table 2 shows the number of fiber measurements required to estimate the mean diameter for two different fiber populations (coefficient of diameter variation is 10% or 50%) with 95% confidence and different error levels. This table indicates that a substantial number of measurements may be required to estimate the mean diameter appropriately. More measurements are required to estimate the coefficient of variation for fibers and even more are required to estimate the diameter distribution.

Figure 7 shows fiber diameter distributions measured for cotton fibers in a thin web when dry, immersed in water and immersed in oil. The figure shows that fiber diameters were larger when wetted in water than when dry or immersed in oil.

Pore structure influences many web properties including filtration performance and fluid flow through webs. Several analytical procedures are used to characterize pore size but little attention has been directed to characterizing the shape and orientation of pores. Figure 8 shows three plots from one set of web measurements to illustrate the detailed information available from image analysis. Figure 8A shows that small pores are oriented in many directions whereas most large pores are oriented toward the MD (MD=0^{o}). Figure 8B shows that the vast majority of small pores are circularly shaped (aspect ratio=1 for circular shape) whereas most large pores are quite elongated. Figure 8C shows that most of the elongated pores are oriented toward the MD.

The orientation directions of fibers in webs can affect many properties, especially mechanical properties. Figure 9 shows fiber orientation distributions for three webs. This figure shows that Web A is most oriented in the MD and Web C is least oriented in the MD.

To test the reasonableness of the fiber orientation distributions shown in Figure 9, theoretical compliance constants were computed from the measured fiber orientation distributions and compared to compliance constants determined experimentally from tensile tests. These are shown in Figure 10 for each of the three webs in Figure 9. Agreement between theoretical and measured compliance is reasonable.

Most web properties as well as variations in web properties are influenced by the uniformity of web structure. It is desirable to characterize total web uniformity as well as uniformity in the machine direction (MD) and cross direction (CD) and to assess uniformity for various size resolutions. This information allows one to characterize web uniformity directionally and for sizes that are most important to a specific web application. We accomplish these goals by providing analysis results in terms of cell-area-dependent web CV% by computing the coefficients of variation among mean gray levels of cells for various cell sizes. That is, an image is divided into many cells of the same size with each cell consisting of n x n pixels and the coefficient of variation is calculated for mean pixel gray levels of the cells. This yields a value of the web CV% for cells of size n x n. When the number n is changed (i.e. cell size is changed), one can obtain data consisting of web CV% versus cell size. We call the corresponding plot a uniformity spectrum and three uniformity spectra are computed - total web, MD and CD by including cells in both image rows & columns, only rows and only columns, respectively. Optical uniformity measurements can be used to compute corresponding basis weight uniformity if calibration data are collected.

Figure 11 shows optical uniformity spectra for two webs. The total uniformity of Web B is slightly better (smaller CV%) than Web A for cell sizes <13mm x 13mm but the total uniformity of Web A is slightly better than Web B for cell sizes >13mm x 13mm. When web uniformity is divided into MD and CD components, a different picture emerges. The MD and CD uniformity's of Web A differ substantially from one another and the web exhibits considerably less CD uniformity than MD uniformity, especially at small size resolutions. This suggests that a problem exists during web formation across but not along the web. Web B exhibits little difference between MD and CD uniformity at all size resolutions.

Figure 12 shows how optical uniformity for the smallest cell size varies with tensile strength and strength variation for four webs. As optical uniformity decreases (CV% increases), tensile strength decreases and tensile strength variation increases.

Summary

In order to understand the properties of nonwoven webs better, increased knowledge of web structure is required. Computer vision techniques can provide this knowledge by detecting and describing web structural features comprehensively. We discussed an instrument featuring powerful multifunction analysis capability, flexible control and automated operation for images acquired at either high or low magnification. The system is economical since six analysis modules share hardware and software resources. Basic hardware and software features of the instrument were discussed and then examples of web structure analysis were provided to illustrate applications.

References

Huang, X.C. and Bresee, R.R. 1993a. Characterizing nonwoven web structure using image analysis techniques. Part I: Pore analysis in thin webs. *Journal of Nonwovens Research,* 5(1), 13-21.

Huang, X.C. and Bresee, R.R. 1993b. Characterizing nonwoven web structure using image analysis techniques. Part II: Fiber orientation analysis in thin webs. *Journal of Nonwovens Research,* 5(2), 14-21.

Huang, X.C. and Bresee, R.R. 1993c. Characterizing nonwoven web structure using image analysis techniques. Part III: Web uniformity analysis. *Journal of Nonwovens Research,* 5(3), 28-38.

Huang, X.C. and Bresee, R.R. 1994. Characterizing nonwoven web structure using image analysis techniques. Part IV: Fiber diameter analysis for spunbonded webs. *International Nonwovens Journal,* 6(2), 53-59.

Inoué, S. 1986. Video Microscopy. Plenum Press, New York.

Yan, Z. and Bresee, R.R. 1999. Flexible multifunction instrument for automated nonwoven web structure analysis. *Textile Research Journal*, 69(11), 795-804.

Table 1. Structure Measured by Web Analysis Instrument.

Pores (thin webs)	Size, shape and orientation distributions Number/unit web area Pore cover percent
Fiber Bundle Diameter	Diameter distribution
Fiber Orientation	Orientation distribution Mean orientation angle MD/CD ratio
Single Fiber Diameter	Diameter distribution Mean and coeff of variation
Basis Weight Uniformity	MD, CD and TOTAL uniformity spectra
Bright & Dark Defects	Size and intensity distributions Number/ unit web area Defect cover percents

Table 2. Number of measurements required to estimate the true mean with 95% confidence

	Maximum Allowable Error		
Diameter CV%	±5 %	±2 %	±1 %
10%	16	97	385
50%	385	2,401	9,604

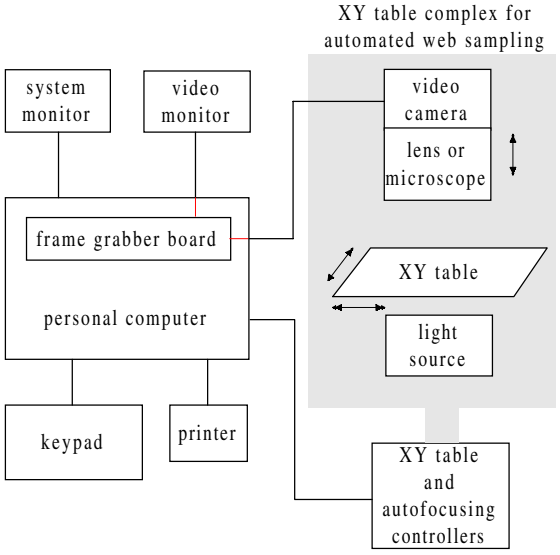

Figure 1. Instrument hardware configuration.

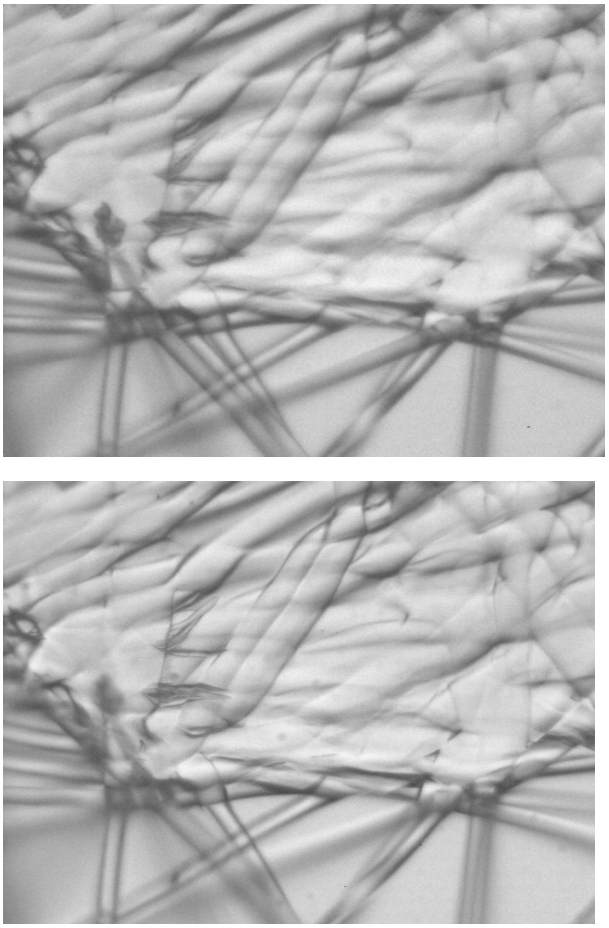

Figure 2. Images acquired with identical λ and NA_{cond} but with (A) NA_{obj} = 0.4 (top) and (B) NA_{obj} = 0.5 (bottom).

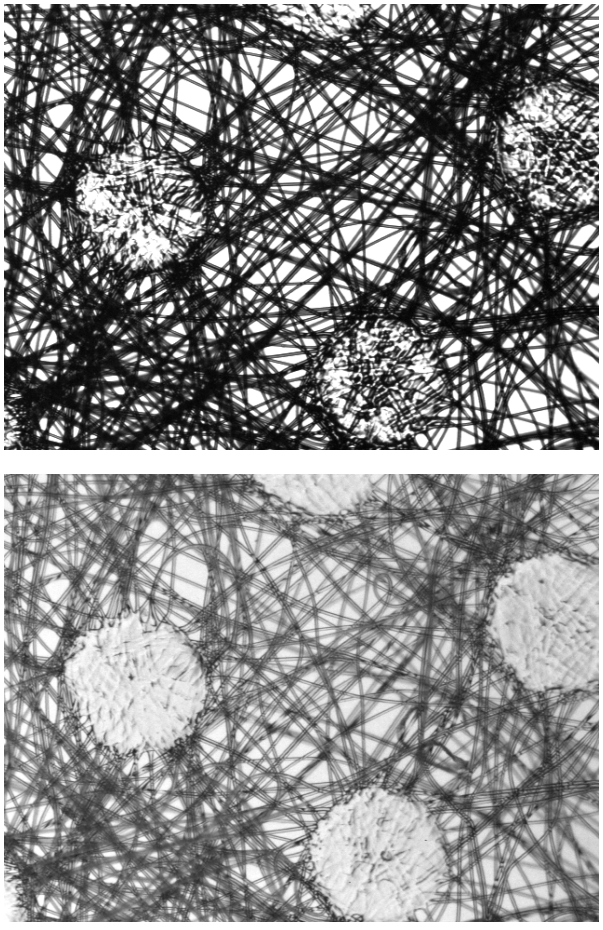

Figure 3. Images acquired with identical NA_{obj} and λ but with (A) smaller NA_{cond} (top) and (B) larger NA_{cond} (bottom).

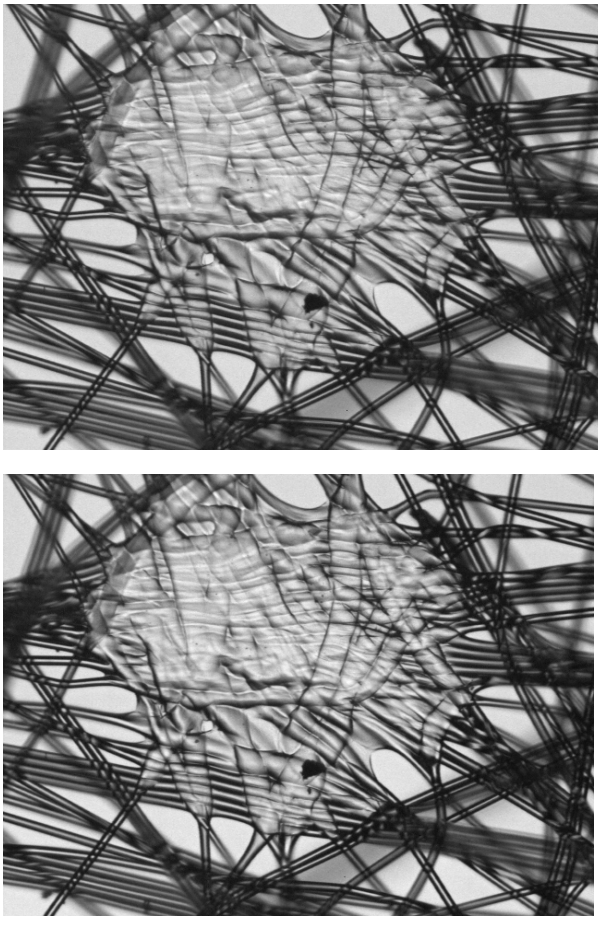

Figure 4. Images acquired with identical NA_{obj} and NA_{cond} but with (A) λ = 486 nm (top) and (B) λ = 656 nm (bottom).

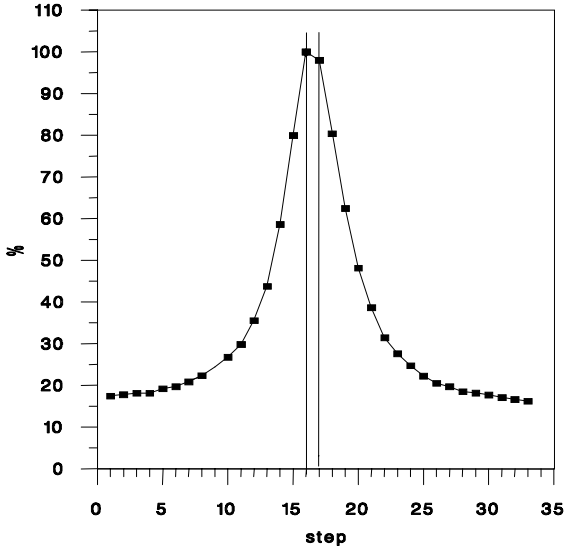

Figure 5. Focus index values for low magnification web images.

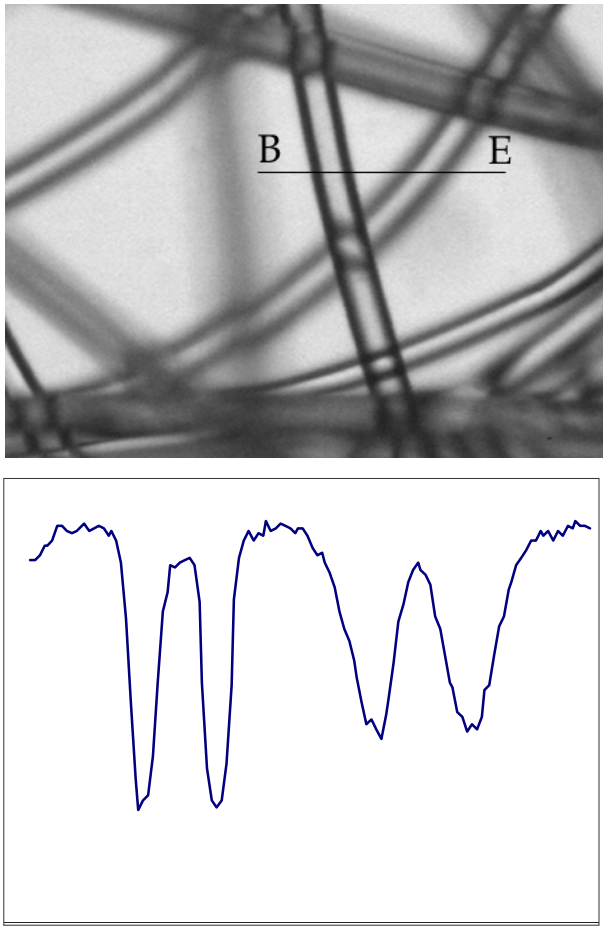

Figure 6. High magnification image: (A) image(top) and (B) gray level pattern (bottom).

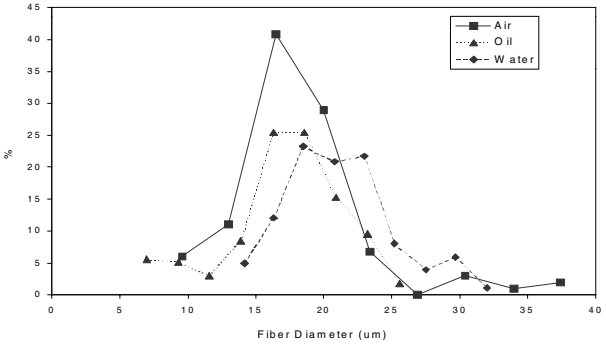

Figure 7. Fiber diameter distributions for cotton when dry, immersed in water and immersed in oil.

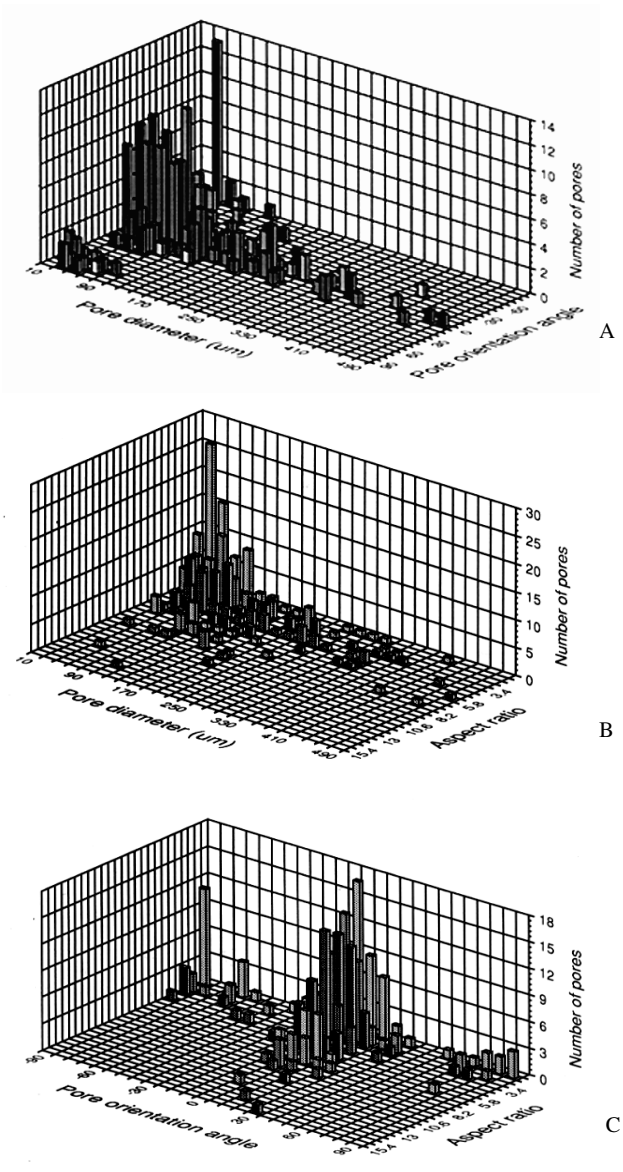

Figure 8. Pore structure: (A) diameter versus orientation angle, (B) diameter versus aspect ratio, and (C) orientation angle versus aspect ratio.

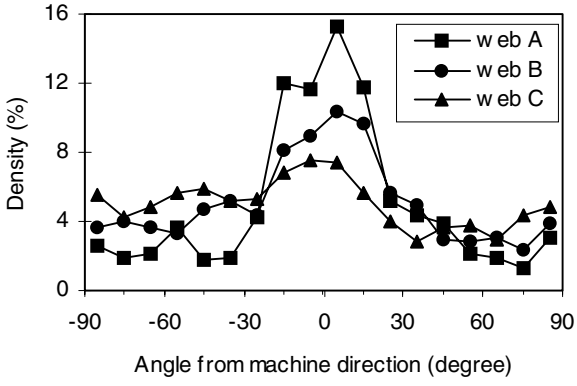

Figure 9. Fiber orientation distributions for three webs.

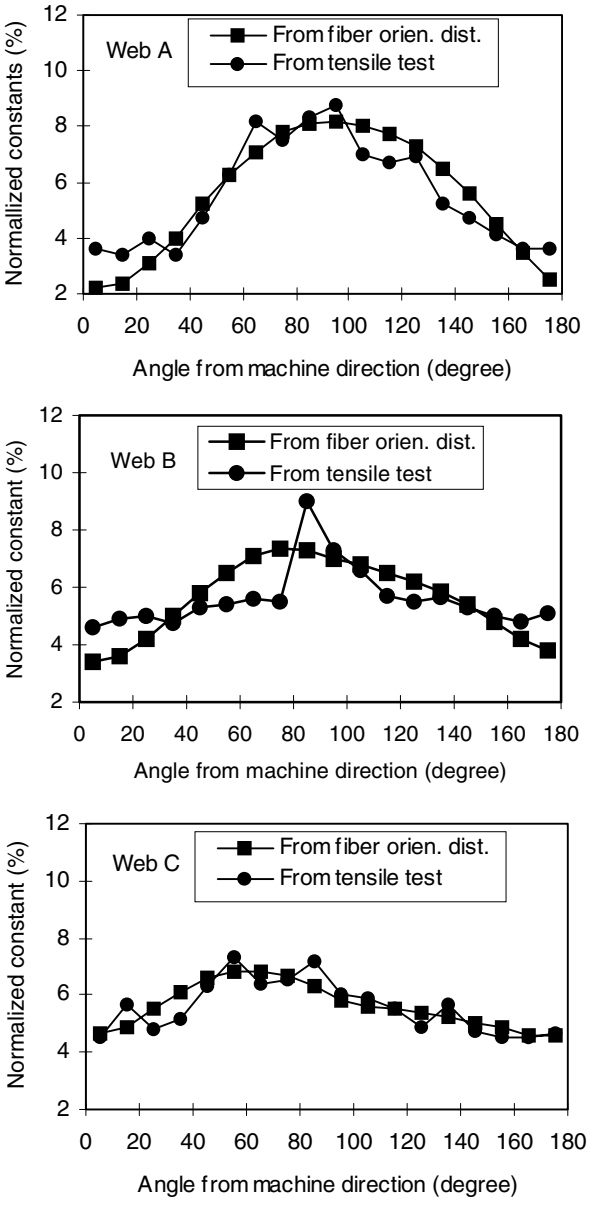

Figure 10. Theoretical and experimentally measured compliance constants for the three webs in Fig. 9.

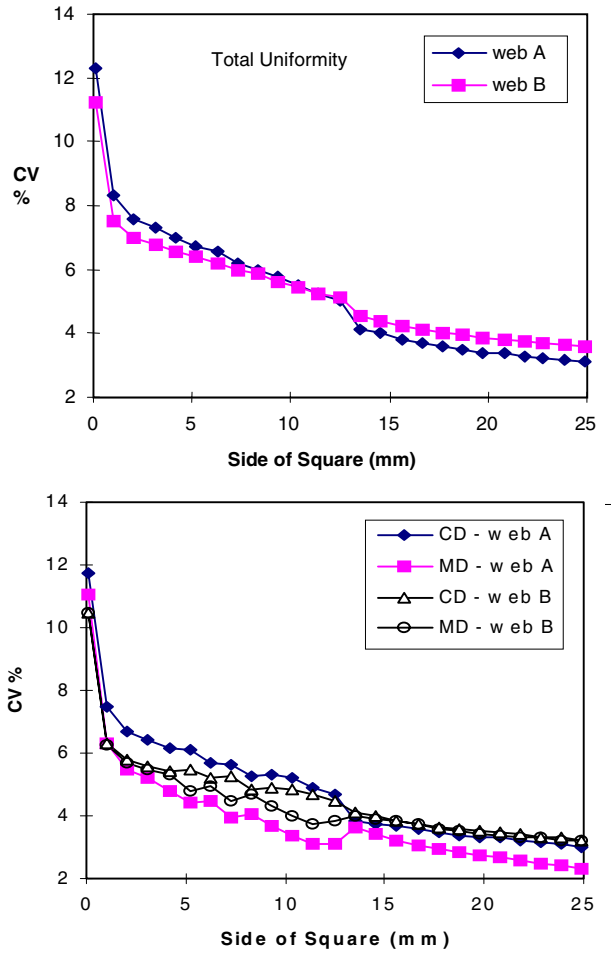

Figure 11. Total uniformity spectra (top) and MD/CD uniformity spectra (bottom).

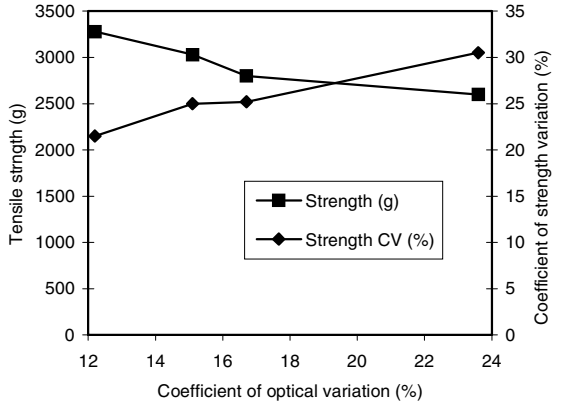

Figure 12. Web optical uniformity versus tensile strength and tensile strength uniformity.